

Development of a High-resolution Fast Gamma-ray Imager for the New-generation PET

Fujio TAKEUTCHI¹⁾

Souichiro AOGAKI²⁾

¹⁾ Faculty of Science, Kyoto Sangyo University,
Kyoto 603-8555 Japan

²⁾ Faculty of Engineering, Kyoto Sangyo University,
Kyoto 603-8555 Japan

I. Introduction

The Positron-Emission Tomography (PET) device based on the current technique is expensive, and this factor, although the device is known to be useful, prohibits the device from becoming popular. We believe that if the read-out method using wave-length shifter is successfully applied to the detection of 511 keV gammas, PET should be produced with a much lower cost. We've been trying a read-out method using wave-length shifter so that many more scintillator crystals are read out with fewer photomultipliers (PM)¹⁾. This allows to use smaller crystals and thus, increases the spatial resolution of detection. We aim at improving it to about 1 mm.

Last year, by using YAP crystals and Kuraray B-2 (800) wave-length shifter, we obtained a spatial resolution of the order of 1 mm (FWHM) for 622 keV gammas from ¹³⁷Cs.

Concentrated effort has been made for one year to clarify the following two points about the read-out of scintillating crystals;

1. How to transport maximum amount of light emitted in the scintillator crystal to the photomultiplier (PM). We tried to understand systematically how the photons are lost at each stage in order to improve the light transmission.
2. How to improve the spatial resolution of the detector. We tried to reproduce in a coincidence measurement the good spatial resolution observed in a measurement with one detector with a collimator.

In addition to the YAP crystal, we made test with LuYAP crystal, and compared the results. The experimental results are presented in the present report. First of all, the components used in the experimental work are explained in this chapter.

1.1 Scintillator crystal

The scintillator crystals used for the detection of 511 keV gamma-ray are YAP(Ce) and LuYAP(Ce). The physical characteristics of these crystals are shown in Table 1.1 together

Table 1.1 Physical properties of the tested scintillator crystals

crystal	YAP(Ce)	LuAP(Ce)	LSO(Ce)
composition	Y Al O ₃	Lu Al O ₃	Lu ₂ Si O ₅
refractive index	1.94	1.95	1.82
density g/cm ³	5.37	8.34	7.35
effective Z	36	65	66.4
decay time ns	25	18	40
yield photons/MeV	14500	9600	27000
wave length nm	370	370	440

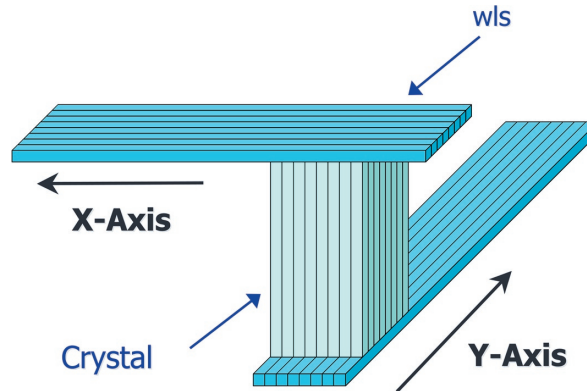
with those of LSO(Ce) which is also going to be tested in the near future.

1.2 Wave-length shifter

The light emitted in the crystal is transported to the PM by means of a light guide. The wave-length shifter (wls) B-2(800) produced by Kuraray company has been used for that purpose. One wls fiber is used to read out many crystals aligned so as to reduce the cost of construction. Fig. 1.1 shows how the x- and y- coordinates of the crystals are read out by the light guides. The wls used has a square section of 1 mm by 1 mm and covered with a single layer clad. The refractive index of the core is 1.59, and that of the clad is 1.49.

1.3 Photomultiplier

The ends of the wls are mounted vertically on the photocathode of 16-channel photomultiplier H6568MOD produced by Hamamatsu Photonics company by means of a small plastic piece in which 16 holes are drilled. Thus 16 wls fibers are connected to one PM.

**Fig. 1.1** Read-out method of the crystals

II. Investigation of the spatial resolution

2.1 Results obtained before this period

2.1.1 Single-detector setup

The ^{137}Cs source has been used as a gamma-ray source. As the scintillator crystals, 1 mm by 1 mm by 20 mm YAP crystals are bundled as a pad (16×16) to form a detector. A 40 mm thick collimator made with lead with a slit of 0.8 mm has been used to select gamma-ray in a small area to be sent to the detector from the source. The distance between the source and the detector was 260 mm.

Fig. 2.1 shows the experimental result obtained with the single-detector setup. The histogram is presented with rectangles whose size represents the yield. Fig. 2.2 shows the projection to the vertical axis of the 2-dim. histogram in Fig. 2.1.

By fitting this histogram with a Gaussian together with a constant background, it was found that the width of the peak is 0.44 channels which means 0.44 mm in RMS. To show that this is not due to an irregularity of a wls fiber nor due to a single channel of PM, we

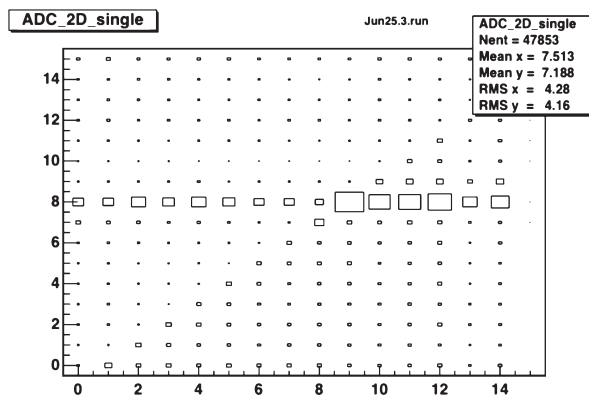


Fig. 2.1 2-dim. histogram of the detected gamma-ray

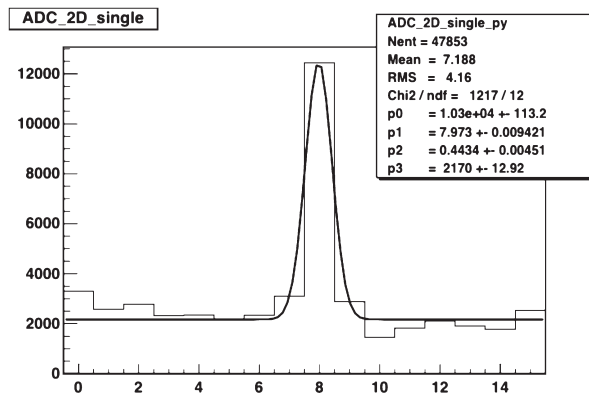


Fig. 2.2 Projection and fit of Fig. 2.1

also did the same test by putting the slit in a diagonal direction, and obtained the similar result. Thus the main component of the detected gamma-ray shows a spatial resolution better than 1 mm in FWHM.

2.1.2 Double-detector setup

As the result obtained above is good, we tried to detect correlated two gamma-rays emitted from a β^+ source by using two detectors. We intended to get rid of the constant background observed in the single spectrum on one hand. On the other hand, it is anyhow necessary to try this set up, which is the part of the configuration used in the real PET. In this study we try to reconstruct the two gamma-rays in coincidence, and extract the spatial resolution in the close-to-real configuration.

Two identical detectors, made of 8×8 crystals are put just on the opposite sides of the source. The β^+ source used is ^{22}Na . The data were acquired with two detectors in coincidence with a time window as wide as 200 ns.

In case the spatial resolution is ideally good, when a crystal in one detector fires, the crystal just on the opposite side with respect to the source point should fire also. In reality, a crystal distant by d crystals from the opposite-side crystal fires in the second detector, this discrepancy d is plotted on the horizontal axis of the histogram shown in Fig. 2.4 obtained with this 2 detector setup.

The shape of the histogram shown in Fig. 2.4 is somewhat peculiar; a Gaussian peak is sitting on a triangular base. We investigate this subject further to understand this histogram.

2.2 Effect of the enlarged source point of the correlated gamma-rays

We expect to find a similar spatial resolution in the experiment with a setup with two detectors also namely of the order of 0.5 mm RMS. If the resolution of the detector does not change in two setups, and if we can rely on the measured resolution at least for the main component, the observed result shown in Fig. 2.4 is difficult to understand. Even we consider only the Gaussian part of the histogram, still the width looks too large. Only way

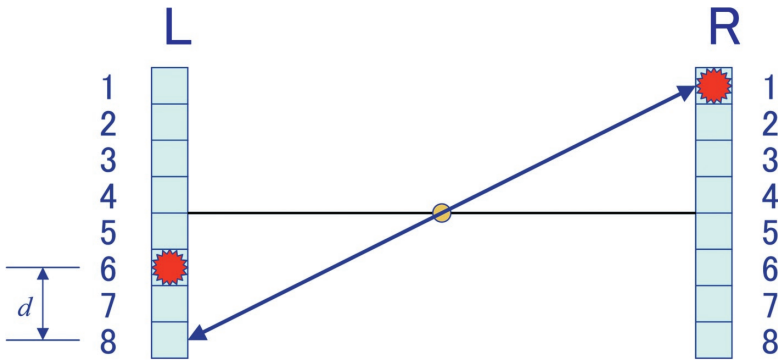


Fig. 2.3 Schematic view of the measurement of the spatial resolution using two detectors

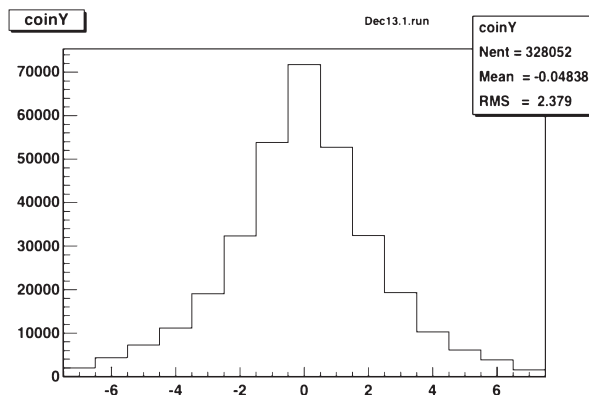


Fig. 2.4 'Discrepancy' d spectrum (see text)

to understand this result seemed to assume that the source of the 2 gamma-rays is actually larger than the β^+ source point which is a bead of 1 mm diameter. If the emitted positron flies a few mm before annihilation, then the histogram could be easily understood. To check this hypothesis, we did the following measurement.

Again we used a single detector, source and a collimator. But this time, the collimator is put near the source as shown in Fig. 2.5. The source point, the slit, and the center of the detector are aligned, for the measurement. Then we shifted the position of the source along the surface of the collimator.

We also measured the histogram for different position of the shifted source. The length of the collimator made from heavy metal is 40 mm, and the opening of the slit is 1 mm. The distance between the source and the detector was 30 cm. The detector consists of 8×8 crystals. The size of the crystals is always the same.

The histogram shown in Fig. 2.6 corresponds to a shift of zero. In this measurement, another detector, put on the opposite side of the source is also used, and the coincidence between two detectors was used as a trigger signal. The width of the broad peak observed was about 2.1 mm (fit parameter $p1$).

Fig. 2.7 shows the result with the source shifted by 0.5 mm. The fitted Gaussian peak has a center outside the shown range ($p1 = 8.298$). Considering the width and the length

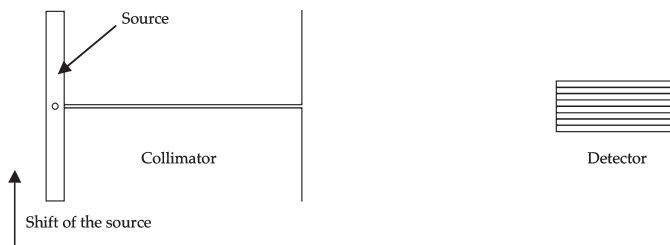


Fig. 2.5 Setup of for the measurement of the size of the source

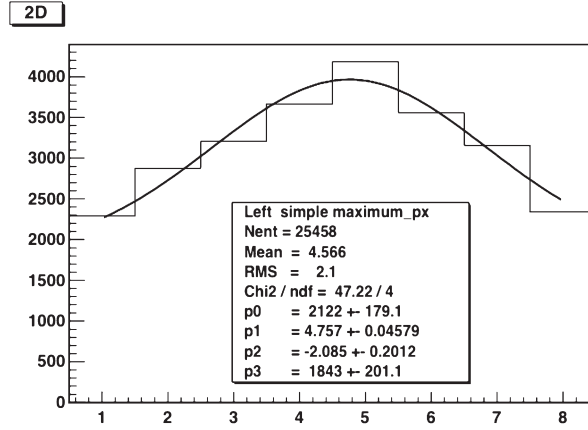


Fig. 2.6 Source position at the center of the slit

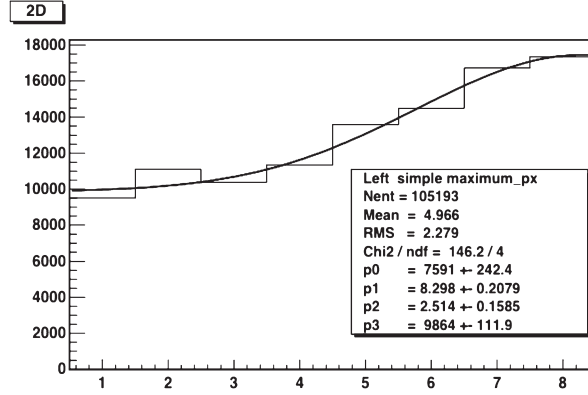


Fig. 2.7 Source shifted by 0.5 mm

of the slit which are 1 mm and 40 mm, and the distance of the detector from the source to be 300 mm, the inclination of tracks is $\sim \pm 4/26$, thus, the result seems reasonable.

To be a little more precise, a simulation study has been performed. The resulting histograms have been fitted using also Gaussians. The histogram shown in Fig. 2.7 has a constant background bias in addition to the Gaussian. The reason for the bias was not known at this stage. Thus the contribution from the gammas going through the collimator was also taken into account. The attenuation of gammas in the collimator material was assumed to be $e^{-0.132747l}$. The origin of the two gammas was assumed to be inside a bead with a diameter of 1 mm. Like in the experiment, the source position was shifted. The positions used in the simulation were, 0, 0.25, 0.5 and 0.75 mm.

First of all, in the simulation, the Gaussian peak is much more prominent compared to the flat background. However, the widths of the Gaussian peaks are almost well reproduced in the simulation. An arbitrary but constant background regardless of the shift was added to the histograms shown in Fig. 2.8 to compare with the measured histograms. It

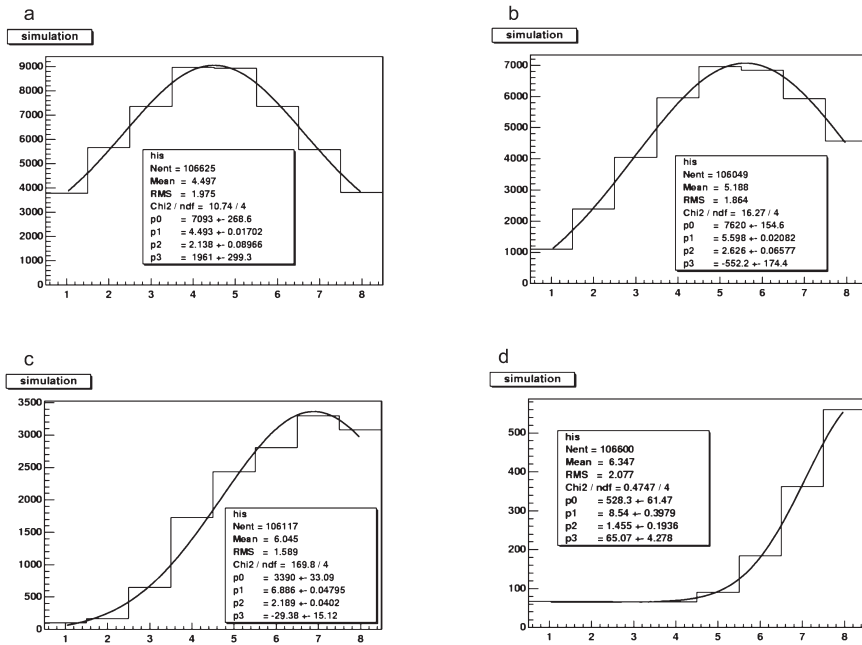


Fig. 2.8 Simulation with the source with shift 0(a), 0.25(b), 0.5(c) and 0.75(d) mm

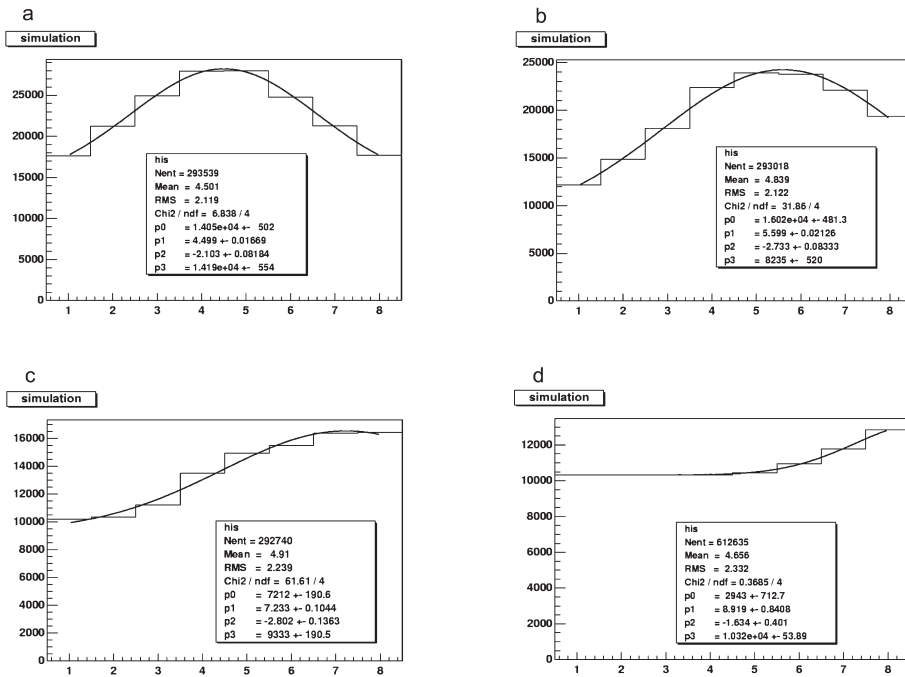


Fig. 2.9 Simulation with the source with shift 0(a), 0.25(b), 0.5(c) and 0.75(d) mm. An arbitrary background was added to the histograms shown in Fig. 2.8 to reproduce approximatively the shape of the measured histograms

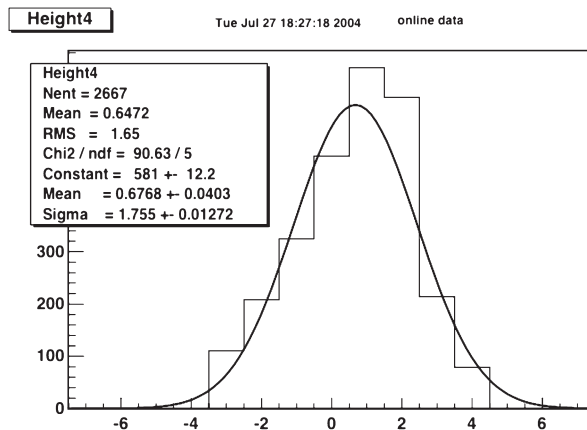


Fig. 2.10 Coincidence-event distribution as a function of the discrepancy d

seems that the simulation results agree fairly well with the observed ones.

Therefore, at this stage, our temporary conclusion is that the successful reproduction with the simulation of the Gaussian peak width probably means that the origin of the two gammas is actually confined in the 1 mm diameter bead.

We then try to extract the spatial resolution of the detector with this set up, namely in the presence of a collimator just next to the source. Again the centers of the two detectors, the source and the slit are all aligned. Fig. 2.10 shows the coincidence-event distribution as a function of the discrepancy d . This histogram seems to contain only a Gaussian, and no triangular bias. The width of the Gaussian peak is about 1.755 mm.

2.3 Background due to the single-gamma radiation associated with the 2 gammas in coincidence from the ^{22}Na β^+ source

The histogram shown in Fig. 2.4 as a function of the discrepancy d seems to have a triangular background in addition to a Gaussian peak. This data has been taken always with a collimator near the source. The triangular background can be understood if there are single gammas emitted randomly and uniformly from ^{22}Na in addition to the correlated pair of gammas. A test was made to check if there is a contribution of the background due to the accidental single gammas.

Two detectors are placed just on the opposite side of the source. Thus if single gammas are detected as contamination, that should show up as triangular distribution in the histogram plotted as a function of the discrepancy d . Thus we removed the coincidence condition from the trigger logic, and positively accepted accidental coincidence events. The result is shown in Fig. 2.11, and this forms a clear triangular shape as expected.

We multiplied an arbitrary number to this distribution, and subtracted from the Fig. 2.4. The result is shown in Fig. 2.12.

A fit using a Gaussian peak gives a width of 1.404, as shown in Fig. 2.13. Assuming that the source is a bead with 1 mm diameter, not a single spot, the peak width must be

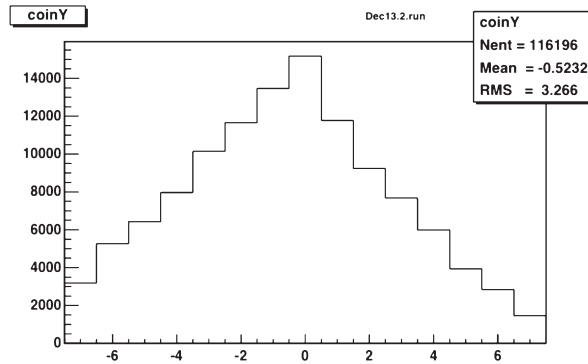


Fig. 2.11 Triangular background due to the accidental coincidence

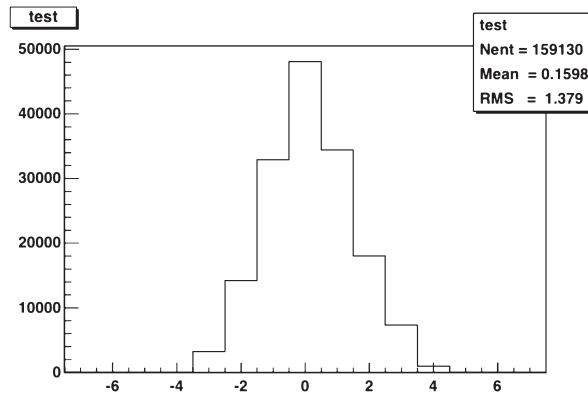


Fig. 2.12 Histogram obtained by subtracting the triangular background

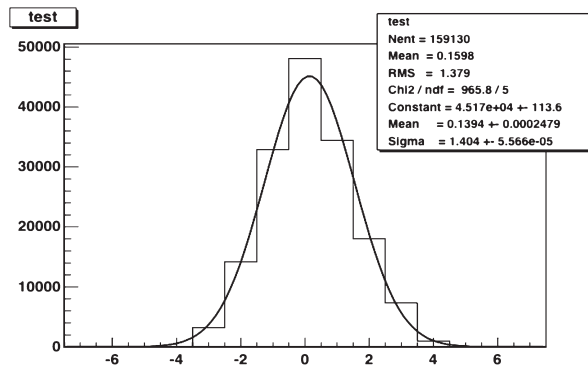


Fig. 2.13 Fit of the data in Fig. 2.12

~ 0.92 mm if the resolution of each detector is 0.4 mm, as measured with the single detector setup. Thus it is 50 % larger than expected.

To conclude, it seems that the contribution from the accidental single gammas is not negligible.

III. Amount of collected light

3.1 Summary of the past experiments

Table 3.1 shows what amount of light is lost at each stage of the light transport from the scintillator crystal to the photomultiplier in the past experiment. This is a result of a simulation in which one million gamma-ray is sent to the crystal. The amount of light produced in the crystal has been calculated using `egs` program²⁾. Then the reflections of the light in the crystal as well as in the wls are simulated using a program written in C++. The size of the crystal is assumed to be $1 \times 1 \times 20 \text{ mm}^3$. The effect of the self-absorption inside the crystal is assumed to be $0.5/\text{cm}^3$. The self-absorption inside LuYAP is not known. We assumed the same attenuation of the light in both crystals.

To improve the amount of collected light, we performed experiments described hereafter.

Table 3.1 Résumé of the number of transmitted photons. `egs` was used to calculate the light emission in the crystal. The number of transmitted photons is calculated at each stage of transmission. The self-absorption effect is included. The colored part corresponds to the case where a silicon rubber is inserted between the crystals and the wls.

	YAP (14500 Photons/MeV)		LuYAP (9600 Photons/MeV)	
	²² Na (551 keV)	¹³⁷ Cs (662 keV)	²² Na (551 keV)	¹³⁷ Cs (662 keV)
Amount of energy transferred to the crystal from gamma	117.255 keV	155.401 keV	189.228 keV	220.414 keV
Photons emitted at the interaction point	1700.198	2253.315	1816.589	2115.974
Number of photons transmitted to the wls (3.732%)	63.449	84.090	67.792	78.965
Number of photons reflected back at the end of the crystal (13.271%)	225.635	299.039	241.081	280.813
Number of photons transmitted from the wls to the photocathode (8.430%)	5.349	7.089	5.715	6.657
Number of photoelectrons obtained (20%)	1.070	1.418	1.143	1.331
Number of photons transmitted to the wls (8.251%)	140.287	185.925	149.890	174.593
Number of photons reflected back at the end of the crystal (8.946%)	152.103	201.586	162.516	189.299
Number of photons transmitted from the wls to the photocathode (8.430%)	11.826	15.674	12.636	14.719
Number of photoelectrons obtained (20%)	2.365	3.135	2.527	2.944

3.2 Study on the self-absorption of the light in the crystal

The light produced in the crystals is read out from both ends of the crystals. According to ref.³⁾, the produced light of 370 nm is absorbed in YAP a half per 1 cm. If that is real, then the strategy to use longer crystals to improve the detection efficiency is not a good one. We made the following test to check this point.

If the self-absorption is large, then a photo absorption or Compton scattering occurring near one end of the crystal produces large amount of light whereas the extracted amount from the other end should be small. Thus we expect a negative correlation between the extracted amount of light from two ends, while if there is no absorption, then the extracted amount of light from an event producing large amount of light should be large at both ends, and should produce a positive correlation.

Fig. 3.1 shows the correlation between the size of the last dynode signal from the x- and y-plane of a detector. Only events with signal outputs from both ends are considered.

The pulse heights correspond only to one or two photoelectrons, and thus it is difficult to find out precisely the correlation. Nevertheless it seems that a negative correlation exists between two planes, and that means that the attenuation effect is rather strong. As described later, we plan to use a silicon rubber between the crystals and wls to increase the amount of lights. We plan to repeat this measurement when the setup is ready.

3.3 Verification of the simulation using a directly mounted crystal

As explained, the loss of the light at each stage of the transfer is fairly large. The simulation study supports the experimentally found result. However, a check is needed about the amount of light produced in the crystal.

A YAP crystal is inserted to the black plastic piece that we usually use to connect the ends of wls to PM, and mounted it directly to the photocathode of a PM as shown in Fig. 3.2. Optical grease has been put between the end of crystal and the photocathode.

Fig. 3.3 shows the obtained pulse-height spectrum together with the fit of the single photoelectron peak (p1).

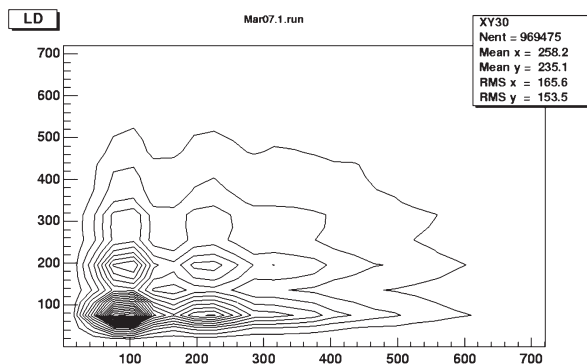


Fig. 3.1 Correlation between pulse-heights at the top and the bottom of crystals

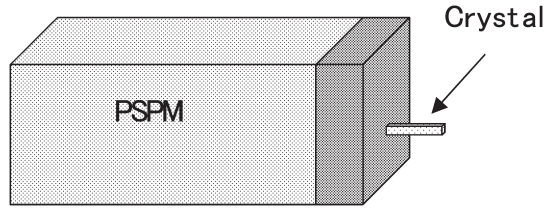


Fig. 3.2 Setup used for the direct measurement of the amount of light from the crystal

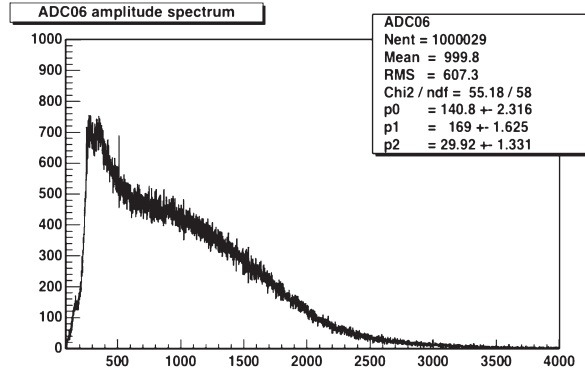


Fig. 3.3 Result of the direct-mounting of the crystal

Table 3.2 Simulated result of the rate of light transmission

	YAP (14500 Photons/MeV)		LuYAP (9600 Photons/MeV)	
	^{22}Na (551 keV)	^{137}Cs (662 keV)	^{22}Na (551 keV)	^{137}Cs (662 keV)
Amount of energy transferred to the crystal from gamma	8.839 keV	11.123 keV	16.763 keV	17.689 keV
Number of photoelectrons obtained	128.162	161.284	160.92	169.816
Number of photons transmitted to the PM (4.79104%)	6.140	7.727	7.710	8.136
Number of photons reflected back at the end of the crystal (18.0548%)	23.139	29.119	29.054	30.660
Number of photoelectrons obtained (20%)	1.228	1.545	1.542	1.627

From this result, one can see that the average number of photoelectrons is 5.94, smaller than the value in Table 3.1. It was found that the reason was that in this experimental setup, the gamma-ray has been sent to the crystal from the side. Thus, to compare with this experimental result, we did another simulation assuming that the gamma-rays come sideways. The result is shown in Table 3.2.

The result shown shows slightly smaller amount of light. But in the above-explained

experiment, the gamma-rays are not always coming perpendicularly, and thus it is normal that this simulation gives a slightly worse result.

Anyhow, it seems that the simulation in the Table 3.1 has been confirmed. We fully understand the loss of light in the current setup.

3.4 Loss of light from the opposite end of the wls

In the above simulation, the efficiency of the wave-length shifter was assumed to be 100 %. Same amount of photons as those transported to the PM are lost at the end of wls which is not connected to PM. We try to save those photons by pasting a piece of aluminized mylar to that end. Improvement of the light collection is checked with this setup.

Fig. 3.4 shows the pulse-height distribution of the last dynode signal in case the piece of aluminized mylar is not yet applied. The position of the single photoelectron peak was found to be 122.8, and the average of the total spectrum is 189.3. Thus the average number of photoelectrons (apparent) is $189.3/122.8$ which is 1.553.

Fig. 3.5 shows the result of the measurement with aluminized mylar. The average number of photoelectrons was found to be $555.2/392$ which is 1.416. No improvement was ob-

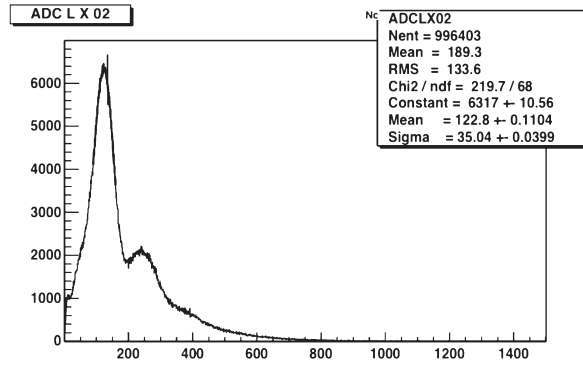


Fig. 3.4 Result obtained in the past

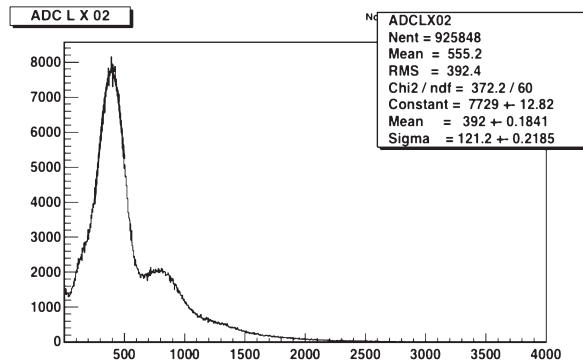


Fig. 3.5 Aluminized mylar used as a reflector

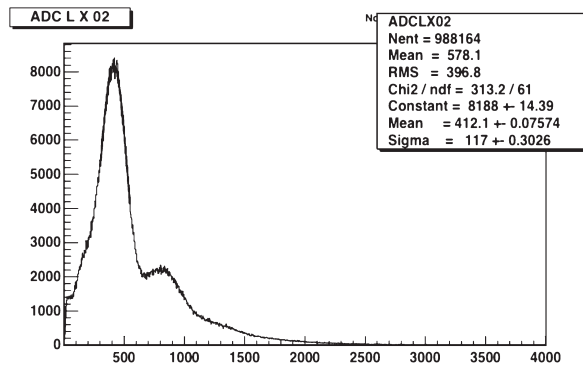


Fig. 3.6 Optical grease applied between the wls and the aluminized mylar

Table 3.3 Result of the application of a reflector

	average number of photoelectrons
none	1.553
with aluminized mylar	1.416
with aluminized mylar and optical grease	1.403

served.

Now, we put a small amount of optical grease between the end of the wls and the aluminized mylar to remove the air gap between them. The result shown in Fig. 3.6 gives an average number of photoelectrons 578.1/412.1 which is 1.403. The result is again worse. The results are summarized in Table 3.3.

Application of aluminized mylar piece to the open end of a light guide was a common practice, and was believed to be efficient so far. We will polish better the end of the wls and try this setup later again.

3.5 Verification of the conversion efficiency of the wls

To confirm the assumption that the conversion efficiency of the light inside the wls is already good, the following test has been performed. The reason for this test is, we observed an improvement of the conversion efficiency when we switched from the dye density from 400 to 800 (Now, 800 is used). A layer of wls was superposed on the normal layer of wls as shown in Fig. 3.7.

We try to find if the amount of light increases when two wls are read in stead of one.

In Table 3.4, the second column shows the average number of photoelectrons observed when only one layer of wls was read. The 3rd column contains average number of photoelectrons when the ADC (charge-sensitive amplitude-to-digital converter) output from two superposed wls are added (see Fig. 3.8). One can observe a slight increase when two layers are read, but the difference is almost negligible. Thus we can conclude that the efficiency of the conversion is almost 100 %.

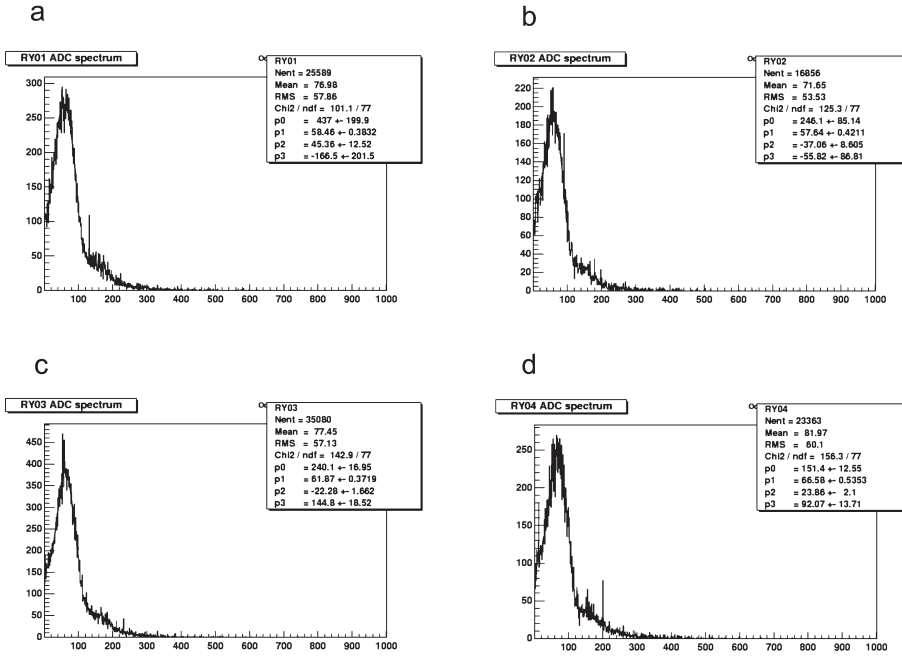


Fig. 3.7 Light output from wls 5(a), 6(b), 7(c) and 8(d)

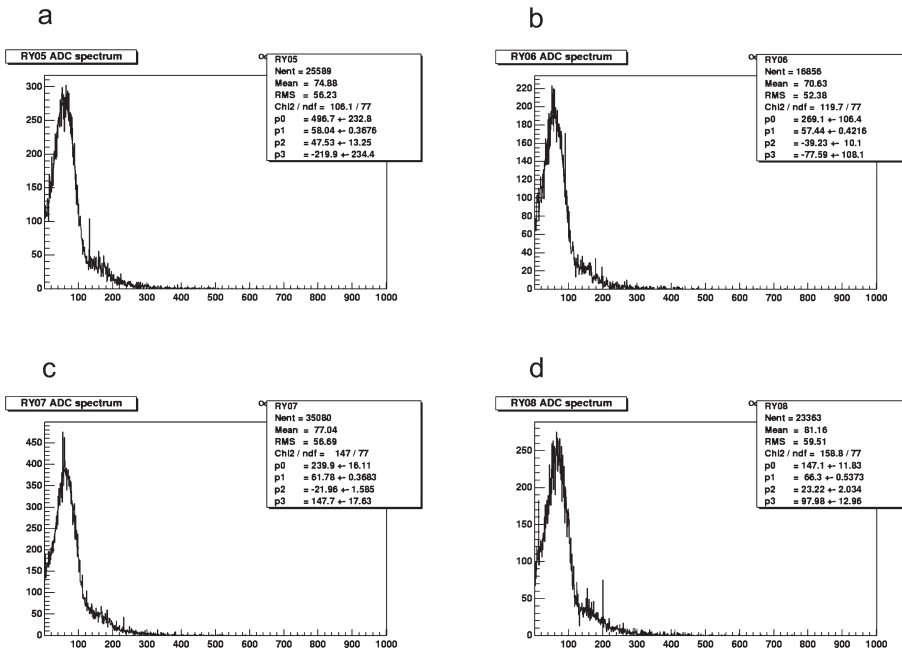


Fig. 3.8 Sum of the outputs from wls 1 and 5(a), 2 and 6(b), 3 and 7(c), 4 and 8(d)

Table 3.4 Light output from single and superposed layers

	First layer only	Sum of 1st and 2nd layers
1	1.29	1.31
2	1.23	1.24
3	1.25	1.25
4	1.22	1.23

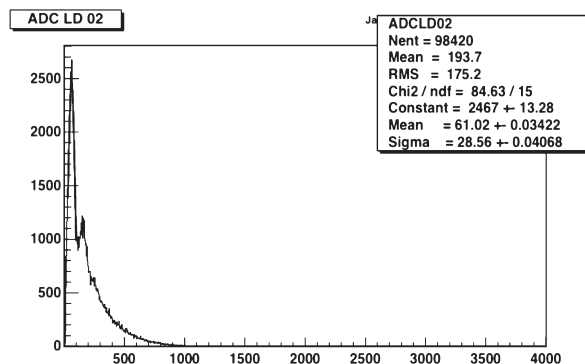
3.6 Removal of the air gap between the crystal and wls

It is known that when the light goes from one material with a lower refractive index to another material with a higher refractive index, insertion of a thin layer with an intermediate refractive index between two materials increases the light transfer. In the current case, the light goes from the scintillation crystal whose refractive index is about 2 to wls whose refractive index is about 1.5 or 1.6, and one cannot use the same technique. However, it is possible that a thin layer of air makes the light transfer difficult, and a removal of this air layer might improve the transfer situation.

A layer of elastic silicon rubber with a refractive index of 1.41, transparent to the near ultra-violet light was inserted as a trial between the crystal and the wls. The results are shown hereafter. For the comparison, the last dynode signal has been used.

Fig. 3.9 shows the ADC spectrum in the setup without the silicon rubber, and Fig. 3.10, with it. The improvement is clear. The single photoelectron peak, very clearly visible, was fitted to find out its position. The average number of photoelectrons (apparent) was calculated by dividing the average of the spectra by the position of the single photoelectron peak position. By inserting the silicon rubber, the average number of photoelectrons changed from 3.174 to 4.489. The piece of silicon rubber we could obtain has a thickness of 1.3 mm, and thus certainly harmful for the spatial resolution. We are now trying to obtain a thinner silicon rubber to be used for this purpose.

To select only events where the light output from the top and the bottom are really from one event, we try to tighten the coincidence time window between the two planes. Fig. 3.11 shows a typical spectrum of the time difference between two discriminator signals. The

**Fig. 3.9** Nothing inserted, just air

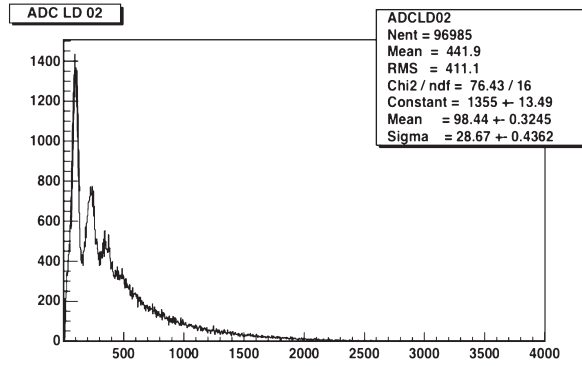


Fig. 3.10 Layer of silicon rubber inserted

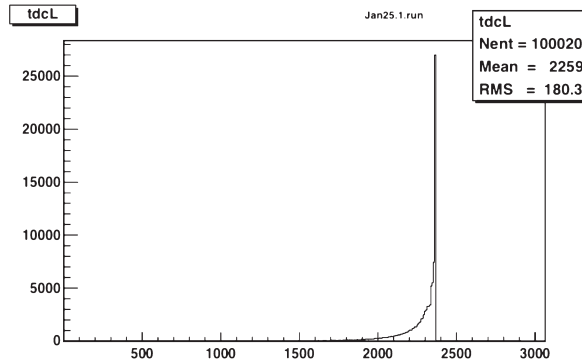


Fig. 3.11 Time difference between x and y plane

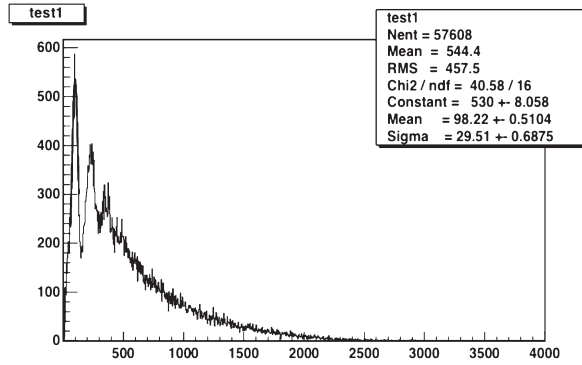


Fig. 3.12 Narrow time window, and with silicon rubber

gain of the spectrum is 122 ps/chan. To test slow crystals, usually the gate width is set to 400 ns. To remove the contribution from the accidental coincidence between two planes, a narrow window of 12.2 ns, namely from channels 2300 to 2400 was applied. The result is shown in Fig. 3.12.

Compared to the case of Fig. 3.10, the number of photoelectrons increases from 4.489 to

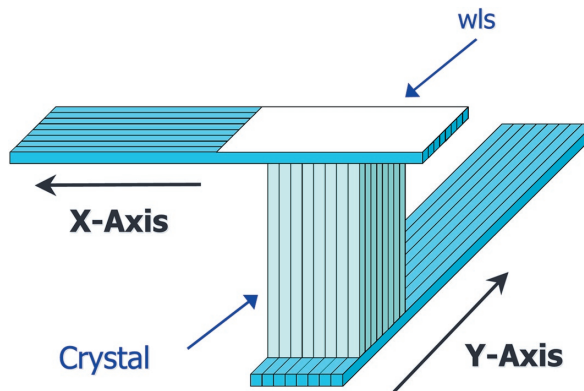


Fig. 3.13 Setup with a reflector

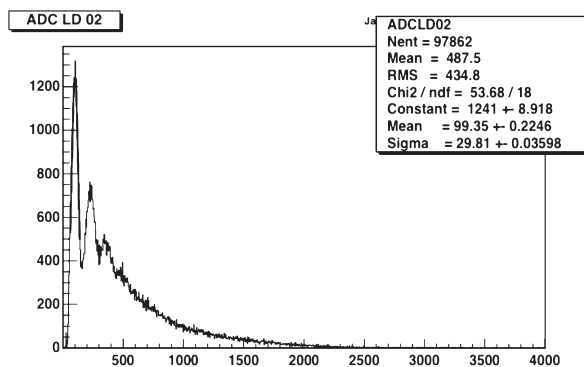


Fig. 3.14 With silicon rubber and a reflector

5.543.

We know that the conversion of the wls of the light coming from the scintillator crystal is almost 100%, nevertheless, we tried a setup with a reflector on top of the wls layer, as shown in Fig. 3.13. The result is shown in Fig. 3.14.

This result is without a narrow TDC window. The average number of photoelectrons increased from 4.489 to 4.907. As expected, the amount of the gain is small, but non-zero.

Fig. 3.15 shows the result of “all effects”, that means with a reflector, and with the narrow TDC (time-to-digital converter) window. The average number of photoelectrons is found to be 5.997, almost 6 which is the best that we can expect for the time being.

As the result was rather positive, we tried the same test using a layer of silicon rubber with the LuYAP scintillator crystal whose light output is rather small. First, Fig. 3.16 shows the spectrum of the last dynode signal from the LuYAP crystal. The average number (apparent) of photoelectrons was calculated to be 1.55.

Next, Fig. 3.17 shows the spectrum with a silicon rubber, and a reflector, and a tight cut on the TDC spectrum. The average number of photoelectrons became 3.051, roughly speaking doubled.

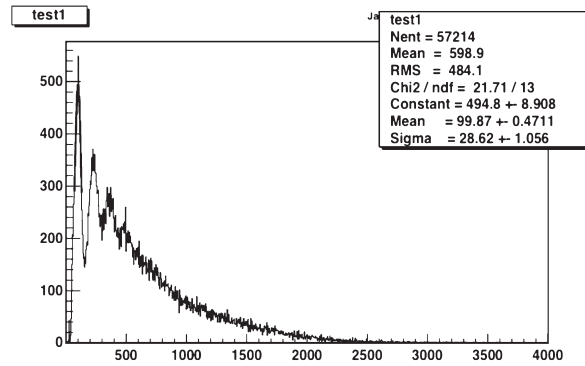


Fig. 3.15 With silicon rubber, a reflector and with a narrow time window

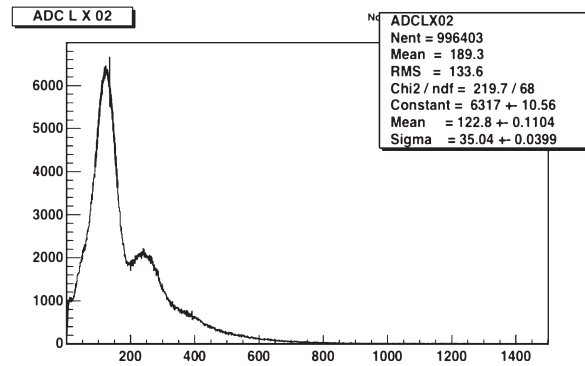


Fig. 3.16 With LuYAP. Nothing inserted, just air

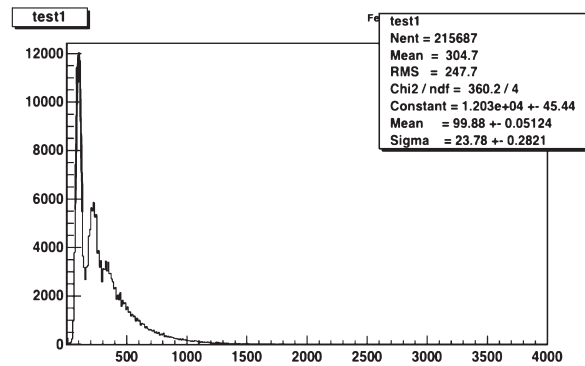


Fig. 3.17 LuYAP: with silicon rubber, a reflector and with a narrow time window

It is clear that a layer of silicon rubber which removes the air between the scintillator crystal and the wls increases the light transfer. Table 3.5 summarizes the result obtained with this test with the YAP crystal.

Of course, we need a thinner layer of silicon rubber to keep the good spatial resolution already obtained. We are now trying to cut the silicon rubber to a thickness of about 0.2

using C4 which determines the time window between two detectors.

4.2 Improvement of the trigger signal

We have been using the LD signal amplified and discriminated as a gate signal for the ADC, and also to form the coincidence between two planes. As the noise in our detection system is small, the threshold of the discriminator has been set to the level of single photoelectron. However, eventually we need to set the threshold to a level of more than one photoelectron. This is not possible with the current setup since the PM and the amplifier are fast (less than 1 ns) while the decay times of the crystals used are much longer (several hundreds of ns). This situation is shown in Fig. 4.3. Thus to be able to set a threshold at higher integrated amount of light, we need some kind of integrator.

Fig. 4.2 show the integrator we inserted in the LD signal. The integrating time was chosen to be about 18 ns.

The bottom figure of Fig. 4.3 schematically shows the output signal of the integration circuit.

Fig. 4.4 shows the real typical signal observed with an oscilloscope.

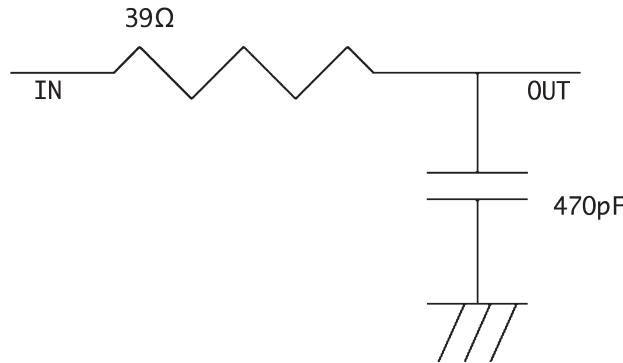


Fig. 4.2 Integrator used. The time constant is 18 ns.

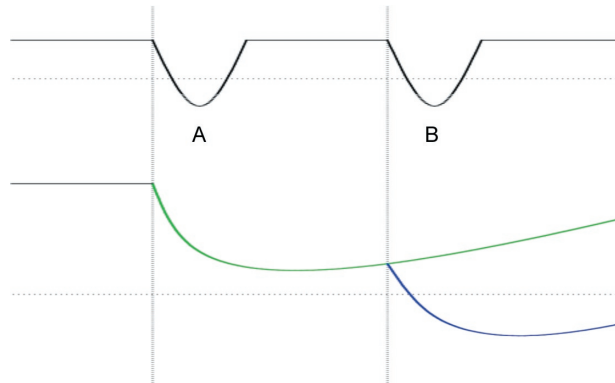


Fig. 4.3 Schematic view of the signals

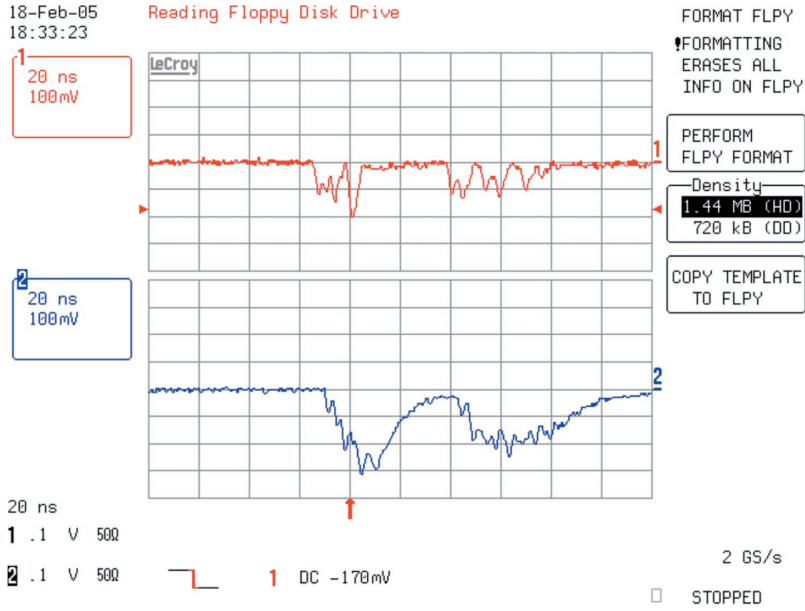


Fig. 4.4 Real signal from the scintillator crystal. Top: raw LD signal from the PSPM. Bottom: After the integrator

The horizontal scale is 20 ns per grid, and vertical scale is 100 mV. The top figure is the raw signal, the bottom signal is the integrated signal.

The signal is from the YAP crystal, and it is shown that the integration time is appropriately chosen. By setting an arbitrary threshold on the discriminator of the LD signal, we can now set an arbitrarily higher threshold. This allows to select large pulse-height events, and also we expect to take data in a little noisier environment.

V. Conclusion

We tried to reproduce the spatial resolution observed with a single detector and a collimator in a set up with two detectors in coincidence. The obtained histogram as a function of the hit position in one detector seemed to show a too wide distribution. Emission of two gammas outside the ^{22}Na source has been suspected, but this did not seem to be the case. Then a coincidence measurement was performed always with a collimator near the source, and a histogram as a function of the discrepancy d was obtained. A Gaussian peak is sitting on a triangular background. We experimentally confirmed that the triangular background is due to the accidental coincidence between two detectors. The Gaussian width of 1.404 mm was obtained by fitting the histogram after an arbitrary amount of triangular background was subtracted.

Removal of the gap between the crystal and the wls by the insertion of a silicon-rubber layer seems to improve drastically the light collection. Together with the modification of the

trigger signal, this can allow one to analyse selectively events with larger pulse heights.

Acknowledgement

The authors would like to thank Prof. M. Toyama for his constant encouragement and help.

This work has been supported by the Grant-in-Aid for Scientific Research 15650107 from Japan Society for the Promotion of Science, the Science Research Promotion Fund from the Promotion and Mutual Aid Corporation for private Schools of Japan, and a grant from Institute for Comprehensive Research, Kyoto-Sangyo University.

References

- 1) F. Takeutchi and S. Aogaki, Read-out of a YAP array detector using wave-length shifter, Proc. Internat. mini - Workshop for Scintillating Crystals and their Applications Nov. 2003, KEK pp. 213–218,
F. Takeutchi, K. Okada and S. Aogaki, Test of non-perturbative QCD by means of the measurement of the K-pi scattering length, Bulletin Inst. Comprehensive Res. Kyoto-Sangyo Univ. I (2003) pp. 15–38,
F. Takeutchi, et al., Test of non-perturbative QCD by means of the measurement of the K-pi scattering length II, Bulletin Inst. Comprehensive Res. Kyoto-Sangyo Univ. II (2004) pp. 1–17
- 2) <http://www.slac.stanford.edu/egs/>
- 3) A. Del Guerra et al., Use of a YAP:Ce Matrix Coupled to a Position-Sensitive Photomultiplier for High Resolution Positron Emission Tomography, IEEE Transactions on nuclear science, Vol. 43, No. 3, June 1996, pp. 1958–1962